Catalysis Today 157 (2010) 211–216

Contents lists available at ScienceDirect

Catalysis Today

journal homepage: www.elsevier.com/locate/cattod

The synthesis of highly crystalline vanadium phosphate catalysts using a diblock copolymer as a structure directing agent

Zhongjie Lin[a], Weihao Weng[b], Christopher J. Kiely[b], Nicholas F. Dummer[a], Jonathan K. Bartley[a,*], Graham J. Hutchings[a]

[a] Cardiff Catalysis Institute, School of Chemistry, Cardiff University, Main Building, Park Place, Cardiff CF10 3AT, UK
[b] Department of Materials Science and Engineering, Lehigh University, Bethlehem, PA 18015-3195, USA

ARTICLE INFO

Article history:
Available online 24 April 2010

Keywords:
Diblock copolymer
Structure directing agent
Vanadium phosphate
PSMA

ABSTRACT

Vanadium phosphate catalysts have been widely studied for the selective oxidation of alkanes to a variety of products including maleic and phthalic anhydride. The synthesis of the precursor is a crucial factor in determining the performance of the final catalyst. Changes in the preparation procedure can alter the morphology, surface area, crystallinity and crucially, the exact vanadium phosphate phases present in the final catalyst which can all affect the selectivity and/or activity of the catalyst. In this study, the use of diblock copolymers in the preparation of phosphate oxidation catalysts has been shown to influence the crystallinity and morphology of the catalyst precursor. By adding a diblock copolymer, poly(styrene-alt-maleic acid) (PSMA), into the preparation uniform, highly crystalline $VOHPO_4{\cdot}0.5H_2O$ precursors are obtained, leading to a faster, more efficient, activation to the active catalyst.

1. Introduction

The controllable synthesis of inorganic materials is important for a variety of applications including medicine, electronics, ceramics, pigments, cosmetics and catalysis. Although particle size control has been realised using a variety of techniques and methodologies, morphological control of particles has proved more difficult to achieve.

A number of catalysts are prepared by chemical reaction including mixed oxides and phosphates. The synthetic procedure for preparing these materials is crucial in controlling properties such as the surface area, the crystallinity, the phases present in the final catalyst and the reproducibility of the performance. Even simple modifications to the preparation method, such as changing the solvent or reducing agent, can have a large effect on the final morphology, the chemical composition and hence, the catalyst performance [1–18].

In the synthesis of microporous materials such as zeolites, the structure is often controlled by the use of a template which can influence the way the material crystallizes and the ultimate structure that is formed. Templates have not been so widely studied for non-zeolitic classes of materials for which they can also be useful synthetic tools.

Biological systems use biomacromolecules, organic molecules that can act as nucleators, cooperative modifiers, matrixes or moulds to aid the morphological control of materials. For example, sea shells, teeth and bones are all made from the same materials but the fine control of nucleation and crystal growth results in unique structures [19–21]. Diblock copolymers have been added as structure directing agents in the synthesis of inorganic materials to try and mimic the effects of the biomacromolecules. One of the most commonly studied copolymers is 2-poly(styrene-alt-maleic acid) (PSMA) which has been investigated as a structure directing agent for a wide range of applications and has been shown to have a variety of different effects depending on the material synthesized.

The use of copolymer structure directing agents has been very commonly applied to the synthesis of semiconductor particles that like catalysts have properties dependent on their shape, size and texture. The morphology of PbS particles has been shown to be dependant on the relative amounts of PSMA and cetyltrimethylammonium bromide (CTAB) added into the preparation mixture [22]. This is proposed to be a result of the structure directing agents preferentially interacting with particular crystal faces of the PbS leading to kinetic control over growth in the [1 1 1] and [1 0 0] directions. Using the PSMA–CTAB mixture star-like PbS particles with six symmetrical, perpendicular arms were formed, but cubic and spherical particles could also be produced if CTAB concentrations were increased.

Diblock copolymers can also be used to promote the crystallization of particular phases, a feature that has been studied for a range of diverse applications, from medicine to improving the strength

* Corresponding author. Tel.: +44 29 2087 0745.
E-mail address: bartleyjk@cf.ac.uk (J.K. Bartley).

0920-5861/$ – see front matter © 2010 Elsevier B.V. All rights reserved.
doi:10.1016/j.cattod.2010.03.013

of cement. Yu et al. showed that PSMA could have an application in preventing urolithiasis [23]. During the formation of CaO_x the addition of the copolymer was found to promote the growth of the tetragonal phase, which is easily expelled from the body, over the monoclinic phase which is difficult for the body to expel and hence, forms kidney stones. The promotion of preferential phases has also been shown to be beneficial in enhancing the characteristics of bulk materials. Adding a polymer into mortar or concrete can significantly improve the properties of the material [24]. Pore structures are improved, workability is increased and water absorption is decreased. When PSMA was added into Portland cement it was found to promote the formation of anhydrous calcium carboxylate over calcium hydroxide which improves the strength of the material [25].

During the preparation of heterogeneous catalysts, preferentially exposing the active plane or preferentially forming the active phase can lead to an increase in selectivity and/or activity. In this study, we show that a diblock copolymer, PSMA, can influence the crystallinity and morphology of a vanadium phosphate catalyst precursor. This is thought to be due to the copolymer acting as a structure directing agent, preventing crystal growth of certain planes and favouring the growth of others. This methodology, although demonstrated for vanadium phosphate catalysts, could be applied to a number of mixed oxide or metal phosphate catalyst preparations to produce more crystalline, uniform catalysts.

2. Experimental

To prepare the standard vanadium phosphate presursor V_2O_5 (5.9 g, Strem) and H_3PO_4 (8.25 g, 85%, Aldrich) were added to isobutanol (2-methyl-1-propanol, 125 ml, Aldrich) and the mixture heated under reflux conditions for 16 h. The resultant pale blue solid was recovered by vacuum filtration, and washed with isobutanol (100 ml) and acetone (100 ml), then dried in air at 110 °C. This material was denoted P0.

For the copolymer modified materials V_2O_5 and H_3PO_4 were reacted in isobutanol with a small amount of Na–PSMA. In a typical preparation, PSMA (sodium salt solution, 13%, Aldrich) was added dropwise to a solution of H_3PO_4 in 15–20 ml of isobutanol under vigorous stirring until a homogeneous solution was formed. The remainder of isobutanol and V_2O_5 was then added and the reaction mixture heated under reflux conditions for 16–18 h. The resultant pale blue solid was recovered by vacuum filtration and dried at 110 °C. Three samples were prepared with different PSMA to V_2O_5 weight ratios of 1:260 (denoted P260), 1:130 (denoted P130) and 1:65 (denoted P65). The precursors P0, P260, P130 and P65 were activated at 400 °C *in situ* in a flow of 1.7% butane in air (150 h for P0, 20 h for P260, P130 and P65) to give their respective catalysts, denoted C0, C260, C130 and C65.

Butane oxidation reactions were carried out in a fixed bed microreactor containing 200 mg of catalyst, at 400 °C with a 3000 h^{-1} GHSV. The feedstock composition was determined to be 1.7% butane/air and controlled by calibrated mass flow controllers. The products were fed via heated lines to an on-line gas chromatograph for analysis. The reactor comprised of a stainless steel tube (i.d. 8 mm) with the catalyst bed held in place by plugs of quartz wool. A thermocouple was located in the centre of the catalyst bed and temperature control was typically ±1 °C. Carbon mass balances ≥95% were typically observed.

The precursor and activated catalyst materials were characterized by a combination of powder X-ray diffraction, BET surface area measurement and electron microscopy techniques. Powder X-ray diffraction (XRD) was performed using a PANalytical X'Pert Pro fitted with an X'Celerator detector and a CuK_α X-ray source operated at 40 kV and 40 mA. BET surface area measurements by nitrogen adsorption at −196 °C were conducted with a Micromeritics Gemini instrument. Scanning electron microscopy (SEM) analyses were carried out on a Hitachi S-4300LV microscope equipped with a Schottky field emission gun. The samples for SEM study were mounted onto an aluminium stub using carbon tape and sputtered with iridium for 30 s to mitigate the effects of sample charging. Samples for transmission electron microscopy (TEM) analysis were prepared by dispersing them in high purity ethanol, and a drop of the resulting suspension was then deposited onto a lacey carbon TEM grid and allowed to dry. Bright field imaging and electron diffraction experiments were carried out using a JEOL 2000FX microscope equipped with a thermionic LaB_6 source operating at 200 kV.

3. Results and discussion

All of the precursor materials were shown by XRD to be the $VOHPO_4{\cdot}0.5H_2O$ phase (Fig. 1). However, a distinct change in morphology can be observed with increasing PSMA concentration. The standard precursor, P0, has the (2 2 0) as the most intense reflection. This decreases with increasing PSMA addition, while the (0 0 1) increases until it is the most intense reflection (Table 1). The different patterns with different relative intensities of the (0 0 1) and (2 2 0) reflections have been previously shown to be characteristic of two distinct morphologies of $VOHPO_4{\cdot}0.5H_2O$ [15–18]. The pattern with the (2 2 0) reflection as the dominant feature is typical of rosette-like structures, whereas the pattern with the (0 0 1) reflection as the dominant feature is typical of rhomboidal platelet structures. The XRD patterns also show that the precursors prepared with PSMA were more crystalline compared with the material prepared using standard procedures, and that the degree of crystallinity improved with increasing PSMA content.

The electron microscopy results correlate with the XRD data. SEM analyses of the precursors show that they are a mixture of characteristic rosette-like agglomerates of angular platelets together with isolated rhomboidal crystallites (Fig. 2). From the micrographs it can be seen that as the amount of PSMA in the preparation was increased the number of rosette-like agglomerates decreased and

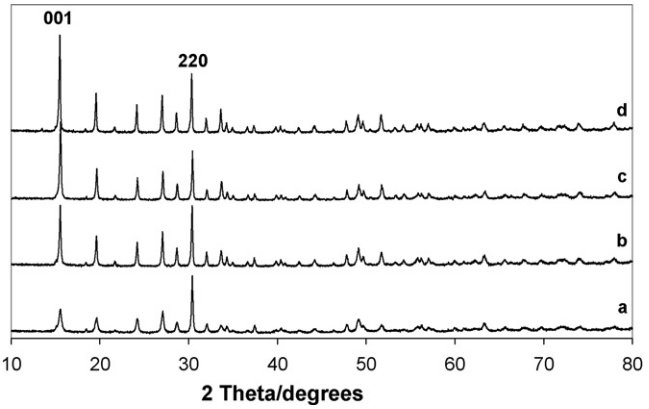

Fig. 1. Powder XRD patterns of: (a) P0; (b) P260; (c) P130 and (d) P65. All reflections can be assigned to $VOHPO_4{\cdot}0.5H_2O$.

Table 1
Relative intensities of the (0 0 1) and (2 2 0) reflections for the $VOHPO_4{\cdot}0.5H_2O$ precursors calculated from the XRD patterns shown in Fig. 1 and BET surface area measurements before and after catalyst testing.

Sample	Relative intensity (0 0 1)/(2 2 0)	Surface area ($m^2\ g^{-1}$)	
		Precursor	Catalyst
P65	1.60	19	21
P130	1.53	13	15
P260	1.01	10	11
P0	0.47	10	12

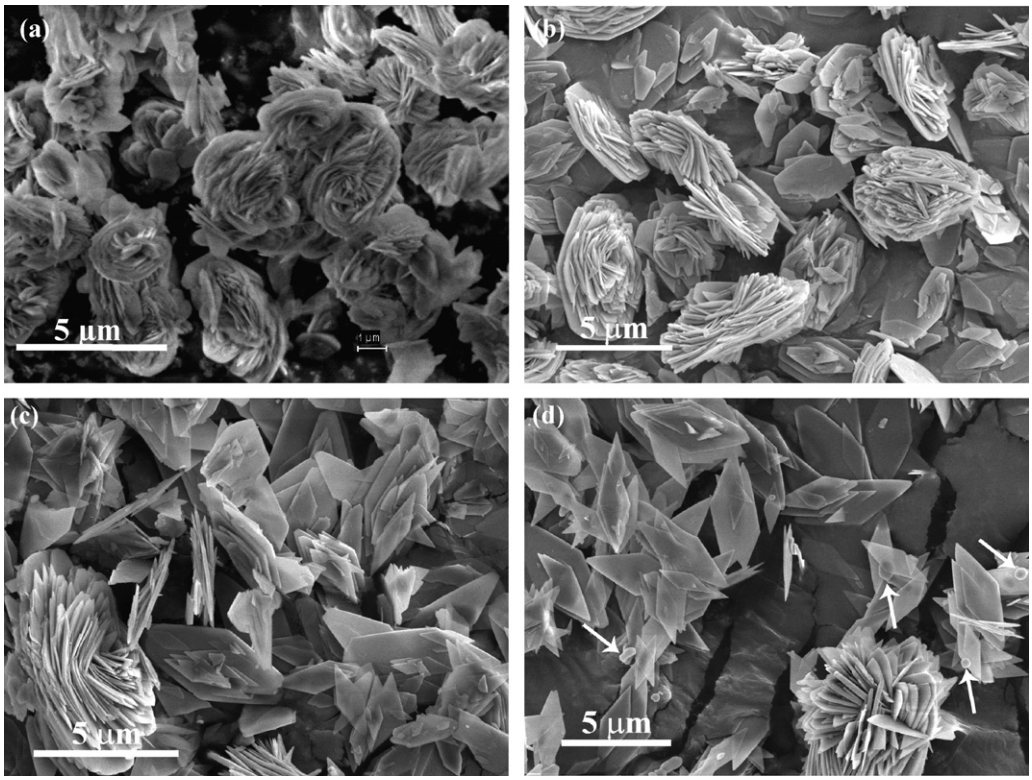

Fig. 2. SEM micrographs of the precursors (a) P260, (b) P130 and (c) P65 (spherical particles are arrowed).

the proportion of rhomboidal platelets increased in agreement with the change in intensity of the (2 2 0) and (0 0 1) reflections observed in the XRD patterns (Fig. 1 and Table 1). For the material prepared with the highest PSMA concentration (P65) there are also a number of small spherical particles which are highlighted by arrows (Fig. 2(d)).

TEM analyses of the rhomboidal platelets are shown in Fig. 3. It can be seen that the crystallites develop more defined morpholo-

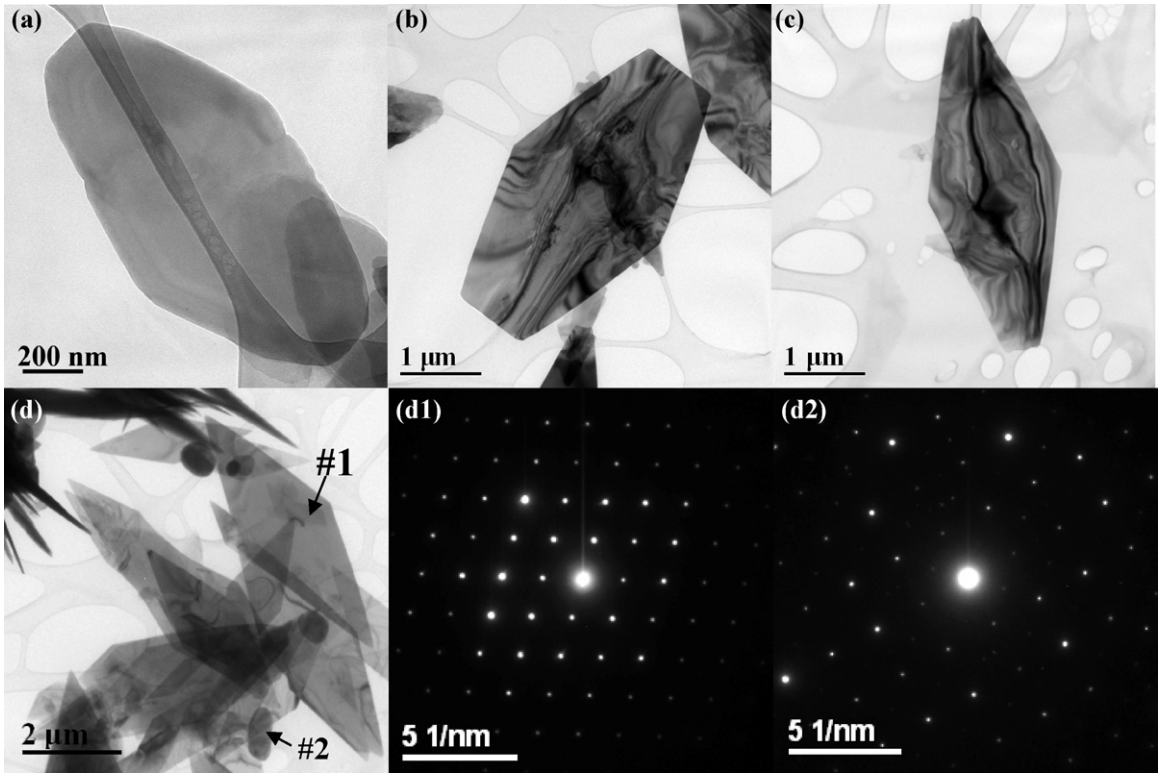

Fig. 3. Bright field (BF) TEM micrographs of the precursors (a) P0, (b) P260 (AR: 1.78), (c) P130 (AR: 2.49) and (d) P65 (AR: 3.00); SADPs from (d1) rhombic platelet (#1 in d) – [0 0 1] $VOHPO4{\cdot}0.5H_2O$ and (d2) sphere (#2 in d) – [0 0 1] $(VO(H_2PO_4)_2)$.

gies as the amount of PSMA is increased. This is in keeping with the proposed mechanisms for how the diblock copolymer acts as a structure directing agent. PSMA consists of two separate monomers as shown below.

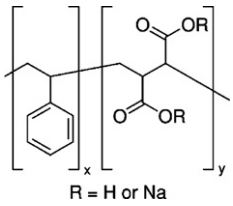

R = H or Na

The styrene group is present to aid solubilization of the polymer in the solvent, whereas the maleic acid group is present to interact with the inorganic material interfaces and crystal planes, giving rise to the structure directing properties. This has been proposed to be due to a specific orientated adsorption of the copolymer onto particular crystal planes, preventing growth in that direction, while promoting crystal growth in the perpendicular planes [22,23,26].

In this study the PSMA seems to promote the formation of the rhomboidal platelets as the number of rosette agglomerations decreases with increasing copolymer concentration. For the material prepared in the absence of PSMA the crystals have rough, ill-defined edges leading to hexagonal particles. When a small amount of the copolymer is added (P260) the hexagonal crystallites become more regular, with well defined edges. The angle between the two long, straight pairs of terminating facets at the platelet edge (Fig. 3(b)) have a characteristic value of 143–144°. These correspond to the (1 4 0) and (1 $\bar{4}$ 0) facet planes of the $VOHPO_4{\cdot}0.5H_2O$ phase. The angle between the flat tip and the platelet edge (1 4 0) facet plane is around 72°, which means this tip corresponds to (1 0 0) facet planes of $VOHPO_4{\cdot}0.5H_2O$. The aspect ratio (AR, length/width) of sample P260 is around 1.78. As the amount of PSMA is gradually increased (P130) the AR increases to around 2.49 (Fig. 3(c)) while the (1 0 0) facet plane becomes jagged. At the highest concentration (P65) the (1 0 0) facet plane disappears and the AR has reached its upper limit at around 3.0 in most of the particles giving four sided, rhombic crystallites (Fig. 3(d)). It is apparent that PSMA can promote the grain growth along {1 4 0} type planes of $VOHPO_4{\cdot}0.5H_2O$. The BET surface area of the samples increases with increasing PSMA addition (Table 1). This is in keeping with the PSMA promoting growth in particular directions leading to thinner platelets giving the material a higher surface area.

Selected area diffraction patterns (SADPs) obtained from these platelets (Fig. 3(a)–(d)) indicated that they were all [0 0 1] oriented $VOHPO_4{\cdot}0.5H_2O$ platelets (one example is shown in Fig. 3(d1)), however, the spherical particles observed at high PSMA concentration were found to be $VO(H_2PO_4)_2$ (Fig. 3(d2)). $VO(H_2PO_4)_2$ is often found as an unwanted impurity phase in the preparation of $VOHPO_4{\cdot}0.5H_2O$ [27], although it can be removed through washing as it is water soluble [28]. It has been previously reported that the production of $VO(H_2PO_4)_2$ is unavoidable due to the reaction with aldehyde formed during the reduction of V_2O_5 with alcohol [13,14]. However, in this study $VO(H_2PO_4)_2$ was only observed with high amounts of PSMA. This could be an indication that there is an optimum amount of PSMA required to form the highly crystalline $VOHPO_4{\cdot}0.5H_2O$ platelets. It is also interesting to note that the $VO(H_2PO_4)_2$ crystallites formed are spherical rather than their usual cubic morphology [13–15]. The formation of spherical particles is common when an excess of the copolymer structure directing agent is added to a preparation and is thought to be a result of the diblock copolymer forming a very strong interaction between the polymer and the crystallizing $VO(H_2PO_4)_2$ which effectively suppresses the crystal growth [29].

When these precursor materials were tested as catalysts for butane oxidation they were found to activate in a very short period of time compared to the standard vanadium phosphate materials (Fig. 4). Typically, the performance of a standard catalyst gradually increases as the $VOHPO_4{\cdot}0.5H_2O$ precursor is gradually transformed *in situ* to the active catalyst ($(VO)_2P_2O_7$ + some V^{5+} phases) over a period of several days before it equilibrates and reaches a steady state performance [30]. The materials prepared with PSMA became active much more quickly and reached a steady state performance in a matter of hours (Fig. 4). This fast activation is attributed to the high degree of crystallinity facilitating the removal of water from the $VOHPO_4{\cdot}0.5H_2O$ lattice during the dehydration step.

The transformation of the active catalyst has been well studied previously and found to be topotactic [16,31]. The characterization of the catalyst after activation confirmed this is the case for the samples prepared using PSMA as can be seen from SEM (Fig. 5) and TEM (Fig. 6) micrographs. The SEM micrographs of catalysts C130 (Fig. 5(a)) and C65 (Fig. 5(b)) show the same features observed in precursor materials P130 (Fig. 2(c)) and P65 (Fig. 2(d)). The activated catalysts consist of a mixture of rhomboidal platelets and rosette-like agglomerates of platelets. The minority spherical particles were found to persist in catalyst C65 which are highlighted by arrows. In the BF TEM micrographs of catalysts C130 and C65 (Fig. 6(a) and (b)) both are found to retain their rhomboidal morphologies after activation and have the similar microstructures, namely interior oblong crystallites and serrated rims (Fig. 6(c)–(f)). Inset SADPs taken from the platelet normal indicate that they are [1 0 0] orientated $(VO)_2P_2O_7$ phase. The angles between the long straight pairs of terminating facets at the platelet edge have a char-

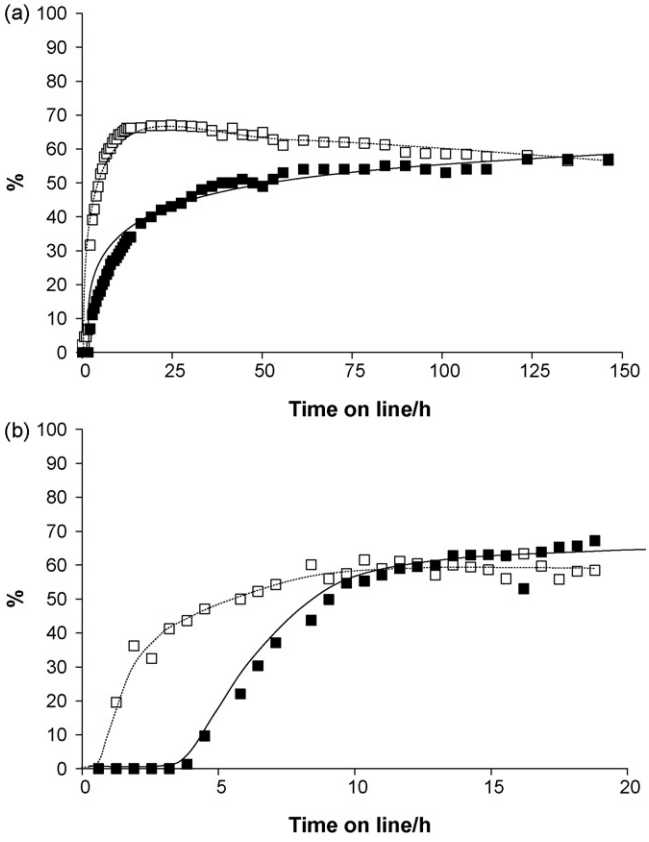

Fig. 4. Butane oxidation over: (a) P0 – steady state performance is reached after >100 h on line; (b) P65 – steady state performance is reached after <10 h on line. (■) Maleic anhydride selectivity; (□) conversion. 1.5% Butane in air, 400 °C, 3000 h^{-1} GHSV.

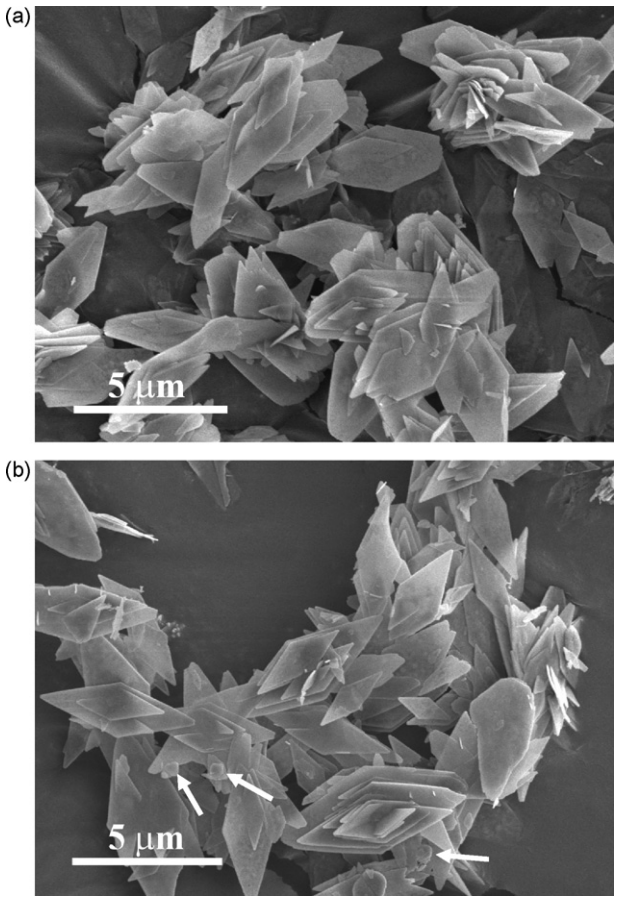

Fig. 5. SEM micrographs of the catalysts: (a) C130 and (b) C65.

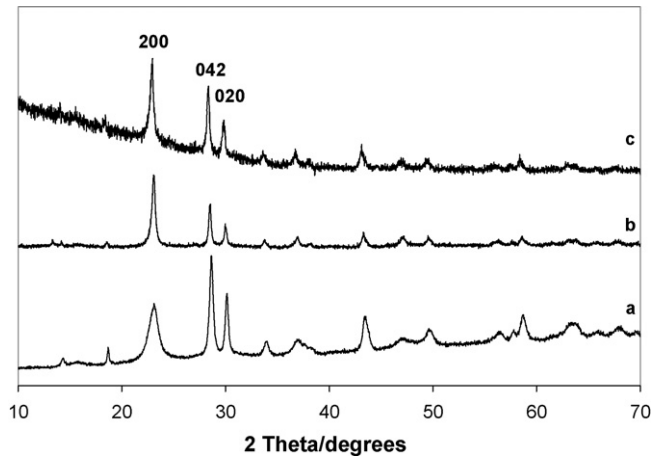

Fig. 7. Powder XRD patterns of: (a) C0; (b) C130; and (c) C65. All reflections can be assigned to $(VO)_2P_2O_7$.

acteristic value of 143–144° as in the precursors, confirming an *in situ* topotactic transformation has occurred.

During the topotactic transformation the [0 0 1] plane of $VOHPO_4{\cdot}0.5H_2O$ becomes the [1 0 0] plane of $(VO)_2P_2O_7$ [31]. The high crystallinity of the precursors prepared using PSMA leads to a $(VO)_2P_2O_7$ XRD pattern with a much sharper and more intense (2 0 0) reflection compared to the standard material (Fig. 7). This intense (2 0 0) reflection is usually only observed when the activation is carried out at high temperature in N_2 [31], and indicates that the final catalyst is much more crystalline for the materials prepared using the copolymer structure directing agent than for the standard material. However, from the TEM studies (Fig. 6) it can be clearly seen that, although the interior of the platelets is crys-

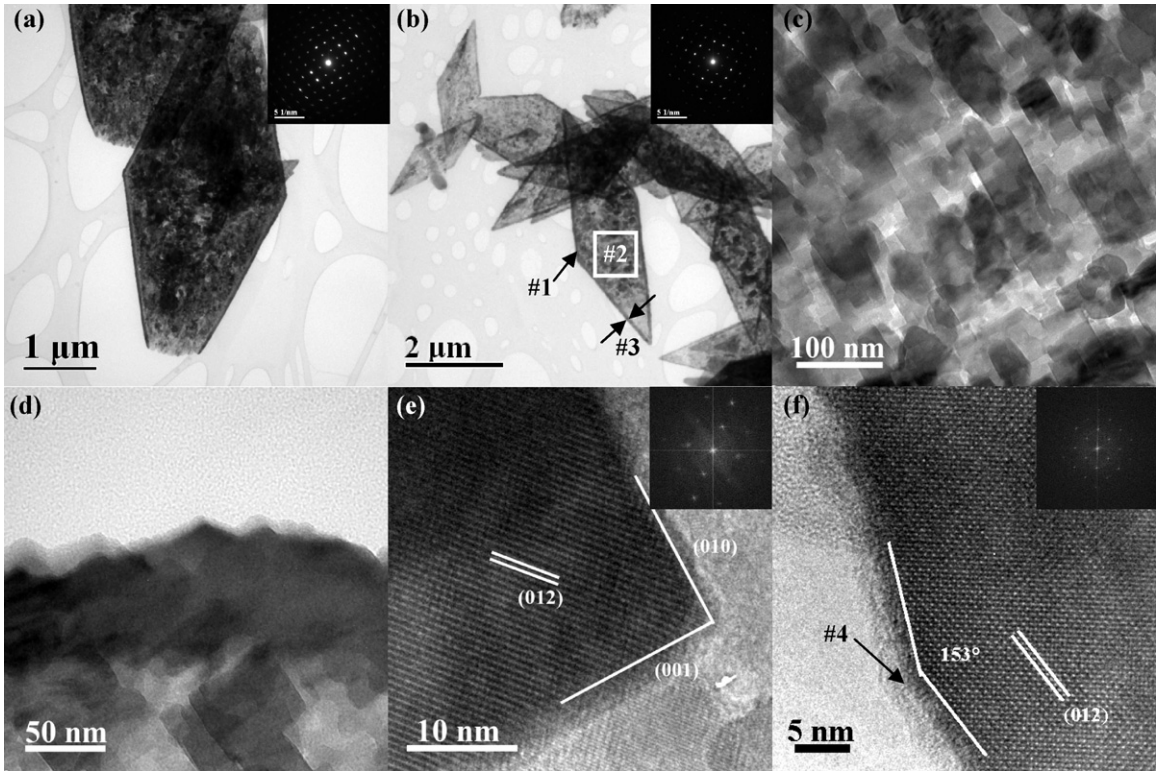

Fig. 6. BF TEM micrographs of (a) activated catalyst C130 {inset SADP from rhomboidal platelet corresponds to [1 0 0] $(VO)_2P_2O_7$}; (b) activated catalyst C65 {inset SADP from rhombic platelet #1 – [1 0 0] $(VO)_2P_2O_7$}; higher magnification BF TEM micrographs of (c) the interior (#2 in b) and (d) rim region (#3 in b) of rhombic platelet (#1 in b); low pass filtered HREM micrographs of (e) small oblong crystallites from area #2 in b showing the [1 0 0] projection of $(VO)_2P_2O_7$ with (0 1 0) and (0 0 1) facet terminations and (f) the serrated rim region (#3 in b) showing characteristic (0 1 2) and (0 $\bar{1}$ 7) facet planes with an intersection angle at around 153° and the disordered overlayer (#4).

talline, an amorphous rim forms around the edge of the platelet. This is in keeping with our previous observations that the active site for butane oxidation is an amorphous overlayer on a crystalline or amorphous bulk support [32–34].

4. Conclusions

Using a diblock copolymer as a template in the preparation of a vanadium phosphate catalyst has been shown to influence the morphology of the synthesized material and also the performance of the activated catalyst. Samples prepared using this methodology were much more crystalline than those prepared using standard methodologies which is attributed to the copolymer template acting as a structure director. It is thought that the template can interact with the (0 0 1) $VOHPO_4{\cdot}0.5H_2O$ plane preventing growth in this direction. This leads to very regular rhomboidal crystals, rather than the lozenge shaped crystals obtained from standard preparations.

For these catalysts the increased crystallinity and morphological changes gives rise to a much faster *in situ* transformation of the precursor to the active catalyst, resulting in a stable steady state performance being reached in a matter of hours as compared to days for the standard catalyst. During the activation of the precursor material there are two processes occurring; the dehydration of $VOHPO_4{\cdot}0.5H_2O$ to form $(VO)_2P_2O_7$ together with a disordering of the surface of the catalyst. The high crystallinity of the precursors prepared using a diblock copolymer template aids the dehydration step, which increases the speed of the activation process before the amorphous surface forms to give the final catalyst.

It is thought that this generic polymer templating methodology can be applied to other catalyst material systems to promote the growth of the desired crystal planes leading to an enhancement in catalytic activity and/or selectivity.

Acknowledgement

We thank the NSF/EPSRC for funding under the Materials World Network Program.

References

[1] J.K. Bartley, I.J. Ellison, A. Delimitis, C.J. Kiely, A.-Z. Isfahani, C. Rhodes, G.J. Hutchings, Phys. Chem. Chem. Phys. 3 (2001) 4606.
[2] J.A. Lopez-Sanchez, J.K. Bartley, R.P.K. Wells, C. Rhodes, G.J. Hutchings, New J. Chem. 26 (2002) 1613.
[3] T. Shimoda, T. Okuhara, M. Misono, Bull. Chem. Soc. Jpn. 58 (1985) 2163.
[4] G. Poli, I. Resta, O. Ruggeri, F. Trifirò, Appl. Catal. 1 (1981) 395.
[5] N. Mizuno, H. Hatayama, M. Misono, Chem. Mater. 9 (1997) 2697.
[6] M. O'Connor, F. Dason, B.K. Hodnett, Appl. Catal. 64 (1990) 161.
[7] F. Cavani, G. Centi, F. Trifirò, Appl. Catal. (1984) 191.
[8] L. Griesel, J.K. Bartley, R.P.K. Wells, G.J. Hutchings, J. Mol. Catal. 220 (2004) 113.
[9] J.K. Bartley, J.A. Lopez-Sanchez, G.J. Hutchings, Catal. Today 81 (2003) 197.
[10] T. Doi, T. Miyake, Appl. Catal. A 164 (1997) 141.
[11] T. Miyake, T. Doi, Appl. Catal. 131 (1995) 43.
[12] N. Guilhaume, M. Roullet, G. Pajonk, B. Grzybowska, J.C. Volta, Stud. Surf. Sci. Catal. 72 (1992) 225.
[13] J.K. Bartley, R.P.K. Wells, G.J. Hutchings, J. Catal. 195 (2000) 423.
[14] J.K. Bartley, R.P.K. Wells, G.J. Hutchings, Catal. Lett. 72 (2001) 99.
[15] I.J. Ellison, G.J. Hutchings, M.T. Sananés, J.C. Volta, J. Chem. Soc., Chem. Commun. (1994) 1093.
[16] J.W. Johnson, D.C. Johnston, A.J. Jacobson, J.F. Brody, J. Am. Chem. Soc. 106 (1984) 8123.
[17] H.S. Horowitz, C.M. Blackstone, A.W. Sleight, G. Teufer, Appl. Catal. 38 (1988) 193.
[18] G.J. Hutchings, M.T. Sananés, S. Sajip, C.J. Kiely, A. Burrows, I.J. Ellison, J.C. Volta, Catal. Today 33 (1997) 161.
[19] S. Mann, Nature 365 (1993) 499.
[20] L.M. Qi, J. Li, J.M. Ma, Adv. Mater. 14 (2002) 300.
[21] L.M. Qi, H. Colfen, M. Antonietti, Chem. Mater. 12 (2000) 2392.
[22] X. Zhao, J. Yu, B. Cheng, Mater. Chem. Phys. 101 (2007) 379.
[23] J. Yu, H. Tang, B. Cheng, X. Zhao, J. Solid State Chem. 177 (2004) 3368.
[24] D.D.L. Chung, J. Mater. Sci. 39 (2004) 2973.
[25] N.P. Singh, N.B. Singh, Prog. Cryst. Growth 52 (2006) 84.
[26] J. Yu, H. Guo, B. Cheng, J. Solid State Chem. 179 (2006) 800.
[27] J.K. Bartley, C. Rhodes, C.J. Kiely, A.F. Carley, G.J. Hutchings, Phys. Chem. Chem. Phys. 21 (2000) 4999.
[28] G.J. Hutchings, R. Higgins, UK Patent 1,601,121 (1981), assigned to Imperial Chemical Industries.
[29] H. Cölfen, L.M. Qi, Chem. Eur. J. 7 (2001) 106.
[30] E.A. Lombardo, C.A. Sánchez, L.M. Cornaglia, Catal. Today 15 (1992) 407.
[31] C.J. Kiely, A. Burrows, G.J. Hutchings, K.E. Béré, J.C. Volta, A. Tuel, M. Abon, Faraday Discuss. 105 (1996) 103.
[32] G.J. Hutchings, A. Desmartin-Chomel, R. Olier, J.C. Volta, Nature 368 (1994) 41.
[33] C.J. Kiely, A. Burrows, S. Sajip, G.J. Hutchings, M.T. Sananés, A. Tuel, J.C. Volta, J. Catal. 162 (1996) 31.
[34] S. Sajip, C. Rhodes, J.K. Bartley, A. Burrows, C.J. Kiely, G.J. Hutchings, in: E.G. Derouane (Ed.), Catalytic Activation and Functionalisation of Light Alkanes, Kluwer Academic Publishers, 1998, pp. 429–433.